

# QUASI-PERIODIC OSCILLATIONS IN THE X-RAY LIGHT CURVES FROM RELATIVISTIC TORI

JEREMY D. SCHNITTMAN<sup>1</sup> AND LUCIANO REZZOLLA<sup>2,3</sup>  
*Draft version November 26, 2018*

## ABSTRACT

We use a relativistic ray-tracing code to analyze the X-ray emission from a pressure-supported oscillating relativistic torus around a black hole. We show that a strong correlation exists between the *intrinsic* frequencies of the torus normal modes and the *extrinsic* frequencies seen in the observed light curve power spectrum. This correlation demonstrates the feasibility of the oscillating-torus model to explain the multiple peaks seen in black hole high-frequency quasi-periodic oscillations. Using an optically thin, monochromatic emission model, we also determine how a relativistically broadened emission line and the amplitude of the X-ray modulations are dependent on the observer's inclination angle and on the torus oscillation amplitudes. Observations of these features can provide important information about the torus as well as the black hole.

*Subject headings:* black hole physics – accretion disks – X-rays: binaries

## 1. INTRODUCTION

Recent observations with the *Rossi X-ray Timing Explorer* (*RXTE*) have revealed the existence of high-frequency quasi-periodic oscillations (QPOs) in a number of accreting black hole binary systems (Strohmayer 2001; McClintock & Remillard 2005). In an increasing number of these systems, the QPOs appear with integer commensurabilities, generally a 2 : 3 frequency ratio (Miller et al. 2001; Remillard et al. 2002; Homan et al. 2005). Since these modulations are expected to originate very close to the black hole, they could be used to test gravity in strong-field regimes or extract information on the black hole properties.

Over the years, a large number of theoretical models have been developed to explain these observations. Some of the more popular models explain the QPOs through magnetic flares (Galeev, Rosner, & Vaiana 1979; Poutanen & Fabian 1999), fluid oscillations in thin disks (Okazaki, Kato, & Fukue 1987; Nowak et al. 1997), geodesic resonances (Stella & Vietri 1999; Abramowicz & Kluzniak 2001), and trapped fluid oscillations in tori around black holes (Rezzolla et al. 2003; Rezzolla, Yoshida, & Zanotti 2003; Montero et al. 2004; Lee, Abramowicz, & Kluzniak 2004; Zanotti et al. 2005).

To evaluate the relative strengths and weaknesses of any of these models, it is essential to compare directly the predictions of the theoretical models with the observations. To this end, we have applied the ray-tracing methods described in Schnittman & Bertschinger (2004) to a numerical calculation of the non-linear dynamics of a relativistic axisymmetric torus described in Zanotti, Rezzolla, & Font (2003). With this combined approach we have calculated the profile of a relativistically broadened emission line, the X-ray light curves, and the power spectra, all as measured by a distant observer. We have demonstrated that a strong correlation exists between the intrinsic normal-mode oscillations of a pressure-supported torus and the extrinsic observables of the X-ray light curves and power spectra. It should be noted that this approach is rather different from the one recently presented by Bursa et al. (2004), where the torus was modeled analytically and thus not the result of self-

consistent relativistic-hydrodynamics simulations.

This Letter is organized as follows: in Section 2 we summarize the basic dynamical features of the perturbed relativistic tori and describe how we apply the classical radiative transfer equation to a general relativistic accretion model. In Section 3 we present simulated images of the torus along with instantaneous line profiles and integrated X-ray light curves for a range of inclinations and perturbation amplitudes, representing the torus initial conditions. We conclude in Section 4 with a discussion of the major results and a look towards future work.

## 2. TORUS DYNAMICS AND RADIATIVE TRANSFER

To briefly summarize the basic properties of the oscillating-torus model, we recall that we are considering a non-self-gravitating perfect-fluid torus orbiting a Schwarzschild black hole (Font & Daigne 2002; Zanotti, Rezzolla, & Font 2003). The fluid is assumed to be in circular non-geodesic motion and the conditions of hydrostatic equilibrium and of azimuthal symmetry allow the relativistic hydrodynamics equations to be reduced to Bernoulli-type equations. These have particularly simple solutions when the fluid is assumed to have a constant specific angular momentum and if a polytropic equation of state is adopted. In this case, the equations of hydrostatic equilibrium can be integrated analytically to yield the rest-mass density distribution inside the torus, with the isobaric surfaces coinciding with the equipotential ones. Hereafter we will consider tori with constant specific angular momentum and bear in mind that more complex distributions introduce only small quantitative differences [see Montero et al. (2004); Zanotti et al. (2005) for details].

Once a stationary equilibrium configuration is constructed, it is perturbed with the introduction of a small radial velocity expressed in terms of the radial velocity for a relativistic spherically symmetric accretion flow onto a Schwarzschild black hole, i.e. the Michel solution (Michel 1972). More specifically, we set the initial radial (covariant) component of the fluid 3-velocity as  $v_r = \eta(v_r)_{\text{Michel}}$ , and then use the dimensionless coefficient  $\eta$  to tune the strength of the perturbation, obtaining an essentially linear response for  $\eta \lesssim 0.06$  (Zanotti, Rezzolla,

<sup>1</sup> Department of Physics, Massachusetts Institute of Technology, 77 Massachusetts Avenue, Cambridge, MA 02139, USA

<sup>2</sup> SISSA, International School for Advanced Studies and INFN, Via Beirut, 2 34014 Trieste, Italy

<sup>3</sup> Department of Physics and Astronomy, Louisiana State University, 202 Nicholson Hall, Baton Rouge, LA 70803, USA

& Font 2003). As noted in Zanotti et al. (2005), the response of the torus is largely independent of the type of perturbation and different choices lead to the excitation of the same modes.

With these initial conditions, the equations of relativistic hydrodynamics in a Schwarzschild black hole space-time are solved using the axisymmetric, general relativistic code described in Zanotti, Rezzolla, & Font (2003) and Zanotti et al. (2005). This makes use of a first-order, flux-conservative formulation of the equations, which are solved using a high-resolution shock-capturing scheme based on an approximate Riemann solver. Second-order accuracy in both space and time is achieved by adopting a piecewise-linear cell reconstruction procedure and a second-order, conservative Runge-Kutta scheme, respectively. As the numerical evolution proceeds, the density and pressure in the fluid’s local rest-frame, as well as the coordinate 4-velocity, are tabulated and stored at each point in space-time.

We recall that the introduction of the perturbations triggers harmonic oscillations of the torus having centrifugal and pressure-gradients as the restoring forces. A careful investigation of these oscillations has also revealed that there are multiple peaks in the power spectrum with frequencies in a sequence of integers:  $2 : 3 : 4 : \dots$  (Zanotti, Rezzolla, & Font 2003; Zanotti et al. 2005). Subsequent perturbative analyses have also shown that these oscillations are indeed  $p$  modes, behaving as trapped waves within the cavity produced by the torus and hence having eigenfrequencies in a sequence of small integers (Rezzolla, Yoshida, & Zanotti 2003; Montero et al. 2004). The striking analogy between the harmonic relation among the  $p$ -mode eigenfrequencies and the QPOs observed in black-hole systems has then led to the suggestion that QPOs could result from basic fluid oscillations of a small accretion torus close to the black hole (Rezzolla et al. 2003). The existence of such tori appears to be a robust feature of global magnetohydrodynamic simulations (DeVilliers, Hawley, & Krolik 2003).

While attractive for its simplicity and for being based on global modes of oscillations that are expected to be present in realistic accretion discs, the relativistic torus model has so far only suggested a property of an orbiting, pressure-supported gas itself. It is not intuitively obvious that “intrinsic” modulations in the fluid hydrodynamics will produce similar “extrinsic” modulations in the observed light curve. Furthermore, it is not clear *a priori* what might be the relationship between the phases and amplitudes of the intrinsic and extrinsic oscillations, and how these might compare with the X-ray data.

To explore this relationship and demonstrate how an oscillating accretion model produces a corresponding oscillating signature in the observed X-ray light curve, we have calculated the trajectories of photons from a distant observer to the emission region around a black hole following the methods described in Schnittman & Bertschinger (2004). In this approach, the photon positions and momenta are tabulated along each ray’s path in order to recreate a simulated, time-varying image of the accreting gas. Given the photon’s 4-position and 4-momentum along the entire path, the observed spectrum is calculated for that ray by integrating the radiative transfer equation with a model for the gas emissivity and absorption.

More precisely, we start from the classical radiative transfer equation (Rybicki & Lightman 1979)

$$\frac{dI_\nu}{ds} = j_\nu - \alpha_\nu I_\nu, \quad (1)$$

where  $ds$  is the differential path length and  $I_\nu$ ,  $j_\nu$ , and  $\alpha_\nu$  are respectively the spectral intensity, emissivity, and absorption co-

efficient of the fluid at a frequency  $\nu$ . These variables are typically defined in the rest-frame of the gas as functions of its local temperature and density. We have explored a number of different emission models, which will be presented in greater detail in a companion paper. For simplicity, the results discussed here are primarily based on an optically thin gas emitting isotropically and monochromatically at frequency  $\nu_{\text{em}}$  with  $\alpha_\nu = 0$  and  $j_\nu \propto \rho \delta(\nu - \nu_{\text{em}})$ .

We then incorporate relativistic effects by defining a local orthonormal tetrad at each point along the integration path (for the Schwarzschild geometry, this is simply the coordinate stationary observer frame). Once transformed to this locally-flat tetrad, only *special* relativistic effects must be included. Following Rybicki & Lightman (1979), equation (1) becomes

$$\frac{dI_\nu}{ds} = \left(\frac{\nu}{\nu'}\right)^2 j'_\nu - \left(\frac{\nu'}{\nu}\right) \alpha'_\nu I_\nu, \quad (2)$$

where primed and unprimed variables are measured in the rest-frame of the gas and in the stationary tetrad, respectively. The special relativistic Doppler shift between the photon path and the fluid can be written as

$$\frac{\nu'}{\nu} = \gamma(1 - \beta \cos \theta), \quad (3)$$

where  $\beta \equiv v/c$ ,  $\gamma \equiv 1/\sqrt{1 - \beta^2}$ , and  $\theta$  is the angle between the photon direction and the gas, all measured in the stationary tetrad. In addition, as the photon bundle propagates through the global curvature around the black hole, the spectral intensity at a given frequency evolves as the photons are gravitationally red-shifted, maintaining the Lorentz invariance of  $I_\nu/\nu^3$ .

### 3. LIGHT CURVES AND POWER SPECTRA

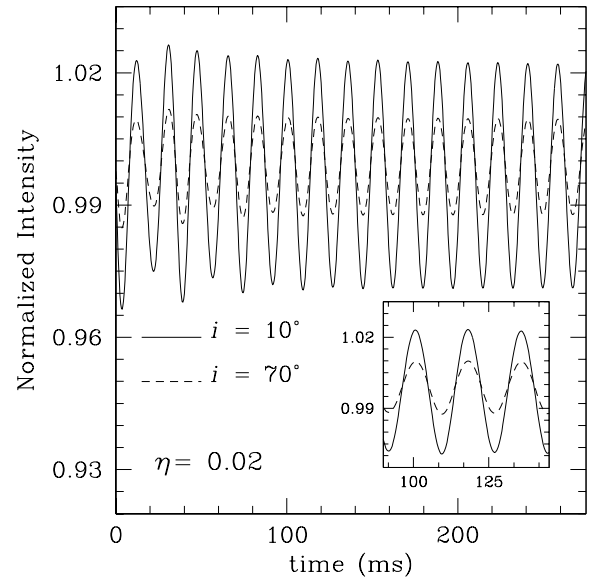


FIG. 1.— Normalized X-ray light curves from oscillating tori with inclinations  $i = 10^\circ$  (solid) and  $70^\circ$  (dashed), for a perturbation amplitude of  $\eta = 0.02$ . The local minima in the light curves correspond to minima in the torus size, when it is closer to the black hole. The inset shows the same light curves in greater detail.

Figure 1 shows the light curves for a torus orbiting around a Schwarzschild black hole of mass  $M = 10 M_\odot$  at inclination angles of  $10^\circ$  and  $70^\circ$ . The amplitude of the initial perturbation was  $\eta = 0.02$ , but qualitatively similar behaviors are seen for

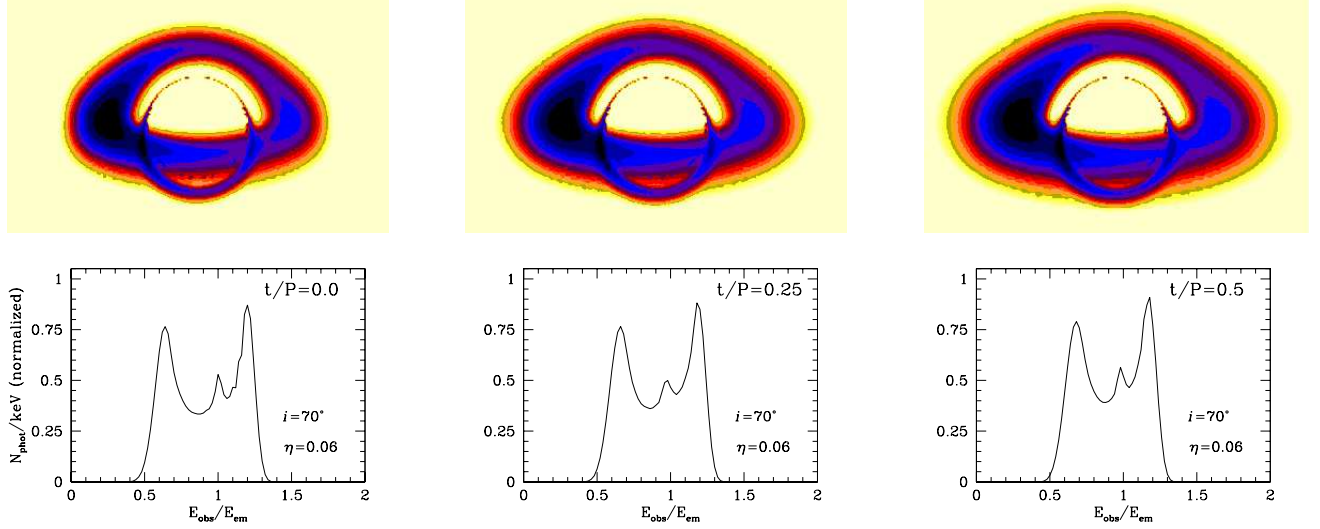


FIG. 2.— *Upper*: Ray-traced images of the oscillating torus, shown at various phases of the fundamental  $p$  mode, with a logarithmic color scale of the X-ray intensity. *Lower*: Broadened emission line spectrum for each frame. The triple-peak spectrum is caused by relativistic beaming towards and away from the observer, along with a central peak due to gravitational lensing of the far side of the accretion torus. The inclination is  $i = 70^\circ$  and the perturbation amplitude is  $\eta = 0.06$ .

perturbations in a linear regime, i.e.  $\delta I/I \propto \eta$  for  $\eta \lesssim 0.06$ , where  $I \equiv \int_0^\infty I_\nu d\nu$ . Although it is clear that the light curve has a quasi-periodic behavior and we find that this is strictly related to the oscillating behavior of the torus at the same frequencies, the modulation of the intensity is the combined result of several different relativistic effects. In particular, for the optically thin emission model, the minimum of the intensity is reached in the “compression” phase of the oscillation, when the torus size is smaller and thus is closer to the black hole. In this case, the gravitational red-shift reduces the observed photon energies (as well as photon number through the invariance of  $I_\nu/\nu^3$ ) as the light has to escape from a deeper potential. At the same time, the intensity is also varied by the special relativistic beaming of photons emitted towards and away from the observer. Finally, smaller contributions to the intensity modulation also come from the transverse (“second-order”) Doppler shift, and from the gravitational lensing of the far side of the torus, magnifying a small region of emission that is moving transverse to the observer (Beckwith & Done 2004; Schnittman, Homan, & Miller 2005).

Because of the conservation of angular momentum during the oscillations, the fluid velocities increase as the torus approaches the black hole, thus enhancing the relativistic beaming of photons toward the observer. For large inclination angles (i.e. when the torus is almost “edge-on”), this beaming is particularly intense and serves to compensate for the intensity decrease due to the gravitational red-shift. As a result, the two major relativistic effects counter each other and the intensity modulation is smaller. For small inclination angles (i.e. when the torus is almost “face-on”), the beaming and gravitational lensing can largely be ignored and the intensity modulation is dominated by the gravitational red-shift and is thus relatively larger (compare dashed and solid lines in Fig. 1). For these smaller inclination angles, simple estimates can be made through the modulated red-shift  $\delta\nu_{\text{obs}} \equiv \nu_{\text{obs}} - \langle \nu_{\text{obs}} \rangle$  and from the invariance of  $I_\nu/\nu^3$ , to obtain  $\delta I/I \approx 3(\delta\nu_{\text{obs}}/\nu_{\text{obs}})$ . The red-shift variation  $\delta\nu_{\text{obs}}/\nu_{\text{obs}}$  is in turn linearly proportional to  $\eta$ .

It is important to underline that the dependence of the modulation of the light curve on the inclination angle is the qualitative opposite of the hot spot model described in Schnittman &

Bertschinger (2004) and could serve to distinguish between the two models as more observations become available. However, because this dependence is a function of the emission model used, further studies are necessary.

In the upper row of Figure 2 we show three snapshots of an oscillating torus at different phases of a single period  $P$ , with  $t/P = 0.0, 0.25, 0.5$ , for a torus with inclination angle  $i = 70^\circ$  and a perturbation amplitude  $\eta = 0.06$ . In the lower row, we show a broadened emission line spectrum for each frame with the typical “multi-horned” features, where the two main peaks are caused by photons emitted towards and away from the observer and thus being blue- and red-shifted respectively. The smaller intermediate peak, on the other hand, is due to the gravitational lensing of the far side of the torus (Beckwith & Done 2004; Schnittman, Homan, & Miller 2005).

When the torus is more compact, closer to the black hole, and the fluid velocities are comparatively larger, the observed emission line is widest as the red-shifted wing moves to slightly lower energies and the blue-shifted wing to slightly higher ones (see panel at  $t/P = 0.0$  in Fig. 2). Furthermore, because of the relativistic invariance of  $I_\nu/\nu^3$ , there are more blue-shifted photons, which increases the total observed flux, compensating in part for the gravitational red-shift of the smaller torus. On the other hand, when the torus is at its maximum size and farther away from the black hole, the blue- and red-shifts in the line spectrum are smaller, but the height of the peaks is comparatively larger (see panel at  $t/P = 0.5$  in Fig. 2).

To quantify more precisely the “quasi-periodicity” in the light curve expected from an oscillating torus, we show in Figure 3 the power spectra from the light curves reported in Figure 1, in units of  $[(\text{rms}/\text{mean})^2 \text{ Hz}^{-1}]$ . The power is clearly dominated by a peak at  $\sim 58 \text{ Hz}$ , which coincides with the lowest  $p$  mode of the torus (indicated as the fundamental  $f$ ). Furthermore, the power spectra also show smaller peaks at the overtones  $o_1 \simeq 3/2f$ ,  $o_2 \simeq 2f$  and  $o_3 \simeq 5/2f$ , thus demonstrating that the light curve possesses the same harmonic behavior of the underlining hydrodynamics.

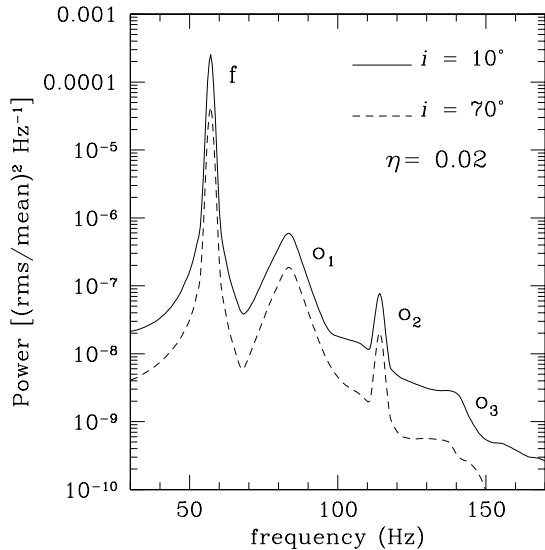


FIG. 3.— Power spectra of the light curves plotted in Figure 1. Note the harmonic ratios among peaks, with  $o_1 \simeq 3/2 f$ ,  $o_2 \simeq 2 f$ , and  $o_3 \simeq 5/2 f$ .

To distinguish between transient modes and the more persistent fundamental oscillations, we have also calculated power spectra for longer time series, corresponding to more than 30 periods of oscillations. In this case we find that the power in the higher modes is reduced and may even disappear if the time series is restricted to the later stages of the oscillations. This result, which is a numerical artifact for low-amplitude perturbations, could however serve as a guide in interpreting the observations. In a real accreting system, in fact, it is likely that any perturbation lasts only a short time, as the turbulent conditions of the accretion disk would continually create and destroy coherent oscillating tori. As a result, these short-lived perturbations could maintain more significant power in the higher harmonics than what was produced with these simulations. Indeed, a characteristic torus lifetime of only 3 – 5 periods is sufficient to explain the observed oscillator quality factors of  $Q \approx 10 - 15$  (Schnittman 2005). Furthermore, the discontinuous phase shift between subsequent tori provides then a natural explanation for the broadening of the QPO peaks and the small changes in frequencies observed as a “jitter” in the peaks.

#### 4. DISCUSSION AND CONCLUSIONS

We have demonstrated the positive correlation between the intrinsic normal mode oscillations of a pressure-supported torus and the extrinsic X-ray light curves and power spectra as seen

by a distant observer. This confirms the feasibility of the oscillating-torus model as an explanation for the integer ratios seen in high-frequency QPO peaks. The specific parameters of the torus model still require further investigation in order to best fit the QPO data.

For the simple emission model considered here, the variation in the light curve is primarily caused by the gravitational red-shift of photons coming from different radii as the torus moves in and out of the black hole’s potential well. Unlike the relativistic hot spot model, the oscillating torus model predicts higher amplitude variations in the light curve for smaller inclination angles, while at higher angles the special relativistic beaming and gravitational lensing counter the gravitational red-shift, reducing the variations in flux. This difference could be crucial to distinguish the two models as more observations become available.

The results reported in this paper serve essentially to demonstrate an issue of principle and have therefore been restricted to a simplified scenario. Even with this advanced analysis tool, we are still limited by the inherent uncertainty in the emission mechanisms and the geometry of the surrounding accretion disk and corona. The fact that the QPOs tend to appear exclusively in the Steep Power Law (“Very High”) state of the black hole and are most significant in the higher energy channels on *RXTE* (McClintock & Remillard 2005) suggests that the specific emission model may be constrained by the features of the X-ray energy spectrum. These spectral features are also important in characterizing the properties of the surrounding thermal disk and hot corona.

Work is in progress to make the results presented here more realistic by analyzing the dynamics of the torus in a Kerr space-time, by considering electron scattering through a corona, and by including optically thick line emission and thermal free-free emission with a Kramer’s opacity law. Initial calculations show qualitatively similar results for the line emission model, but the thermal emission model predicts a “phase inversion” with respect to the light curves shown in this paper. This is due to the fact that for a barotropic equation of state the temperature increases at smaller radii when the density and pressure increase. This higher temperature produces greater X-ray emission, outweighing the gravitational red-shift of the smaller radius. These results will be presented in greater detail in a forthcoming paper.

JDS is grateful to Edmund Bertschinger for his insights and encouragement. Helpful discussions with Olindo Zanotti are also acknowledged. Support comes by NASA grant NAG5-13306.

#### REFERENCES

- Abramowicz, M. A., & Kluzniak, W. 2001, *A&A*, 374, L19  
 Beckwith, K., & Done, C. 2004, *MNRAS*, 352, 353  
 Bursa, M., Abramowicz, M. A., Karas, V., & Kluzniak, W. 2004, *ApJ*, 617 L45  
 De Villiers, J.-P., Hawley, J. F., & Krolik, J. H. 2003, *ApJ*, 599, 1238  
 Font, J. A., & Daigne, F. 2002, *MNRAS*, 334, 383  
 Galeev, A. A., Rosner, R., & Vaiana, G. S. 1979, *ApJ*, 229, 318  
 Homan, J., et al. 2005, *ApJ*, 623, 383  
 Lee, W. H., Abramowicz, M. A., & Kluzniak, W. 2004, *ApJ*, 603, L93  
 McClintock, J. E., & Remillard, R. A. 2005, in *Compact X-ray Sources*, ed. W. H. G. Lewin & M. van der Klis, preprint (astro-ph/0306213)  
 Michel, F. 1972, *Astrophys. Spa. Sci.*, 15, 153  
 Miller, J. M., et al. 2001, *ApJ*, 563, 928  
 Montero, P. M., Rezzolla, L., Yoshida, S’i., 2004, *MSRAS*, 354, 1040  
 Nowak, M. A., Wagoner, R. V., Begelman, M. C., & Lehr, D. E. 1997, *ApJ*, 477, L91  
 Okazaki, A.T., Kato, S. & Fukue, J., 1987, *PASJ*, 39, 457  
 Poutanen, J., & Fabian, A. C. 1999, *MNRAS*, 306, L31  
 Remillard, R. A., et al. 2002, *ApJ*, 580, 1030  
 Rezzolla, L., Yoshida, S’i., Maccarone, T. J., & Zanotti, O. 2003, *MSRAS*, 344, L37  
 Rezzolla, L., Yoshida, S’i., & Zanotti, O. 2003, *MSRAS*, 344, 978  
 Rybicki, G. B., & Lightman, A. P. 1979, *Radiative Processes in Astrophysics* (New York: Wiley-Interscience)  
 Schnittman, J. D., & Bertschinger, E. 2004, *ApJ*, 606, 1098  
 Schnittman, J. D. 2005, *ApJ*, 621, 940  
 Schnittman, J. D., Homan, J., & Miller, J. M. 2005, submitted to *ApJ*  
 Shakura, N. I., & Sunyaev, R. A. 1973, *A&A*, 24, 337  
 Shapiro, S. L., Lightman, A. P., & Eardley, D. M. 1976, *ApJ*, 204, 187  
 Stella, L., & Vietri, M. 1999, *Phys. Rev. Lett.*, 82, 17  
 Strohmayer, T. E. 2001, *ApJ*, 552, L49  
 Zanotti, O., Rezzolla, L., & Font, J. A. 2003, *MNRAS*, 341, 832  
 Zanotti, O., Font, J. A., Rezzolla, L., & Montero, P. M., 2005, *MSRAS*, 356, 1365